Phenol Adsorption and Photo-oxidation on Porous Carbon/Titania Composites[†]

Leticia F. Velasco[*], José B. Parra and Conchi O. Ania *Instituto Nacional del Carbón, (INCAR-CSIC), C/Francisco Pintado Fe, 26, 33011 Oviedo, Spain.*

ABSTRACT: Carbon/titania composites with different loadings were prepared and investigated for phenol adsorption and photo-oxidation from dilute aqueous solutions. The rate of phenol adsorption increased when titanium oxide (P25, Degussa) was immobilized on the carbon support due to the porous features of the resulting C/TiO_2 composites. The kinetics of phenol adsorption were very fast for samples containing low titanium oxide contents, whereas titania loadings above 20 wt% presented some operational problems that prevented their application in aqueous solutions. Those C/TiO_2 composites which exhibited higher adsorption rates in the absence of illumination also showed a more rapid disappearance of phenol from aqueous solution under UV light, together with the formation of lower amounts of intermediates. Removal efficiencies close to 100% were obtained for C/TiO_2 composites containing ca. 10–15 wt% titanium oxide, with preferential oxidation of phenol through the formation of catechol.

1. INTRODUCTION

In recent years, considerable interest has arisen in the development of advanced and more efficient procedures for wastewater remediation, driven by the drawbacks of conventional technologies (i.e. reverse osmosis, ion-exchange resins and adsorption) in dealing with persistent aromatic compounds. Poor economic feasibility, limited applicability and effectiveness, and a short lifetime due to low regeneration capacities are among the most important limitations of conventional technologies for water treatment.

In this respect, photocatalytic degradation is a promising technology for the removal of toxic pollutants from water, with titania (TiO_2) being the most commonly used photocatalyst because it is non-toxic, photo-stable, cheap and very efficient under UV light irradiation (Pelizzetti and Serpone 1989). However, nano-sized titania powders present some operational problems (recovery and re-use of the catalysts) that make the large-scale implementation of this technology difficult. For this reason, the immobilization of the photoactive powder on different supports is being widely investigated (Mohseni 2005; Fernández *et al*. 1995; Bideau *et al*. 1995).

Thus, the immobilization of titanium oxide on carbon supports has currently attracted much attention for the photodegradation of organic pollutants (Tryba *et al*. 2003; Keller *et al*. 2005; Velasco *et al*. 2010; Matos *et al*. 2001, 2007). The photo-activity of carbon/titania composites depends strongly on the properties of the carbon material used as the support, the dispersion of titania on the porous support and the titania/carbon loading. Indeed, it has been reported that the

[†]First presented at the XXXVth Iberian Adsorption Meeting (RIA – Reunião Ibérica de Adsorção), Lisbon, Portugal, 8–10 September, 2010.

[*]Author to whom all correspondence should be addressed. E-mail: leticia@incar.csic.es (L.F. Velasco).

presence of carbon actually changes the catalytic behaviour of TiO_2 beyond a synergistic effect on the degradation kinetics (Velasco *et al*. 2010, Araña *et al*. 2003a,b).

On the other hand, immobilization of TiO_2 on a porous substrate is expected to yield a photocatalyst with a higher activity, since the porous support promotes contact between the catalyst and the substrate (adsorbate) via adsorption. This is important because the photo-generated oxidizing species (•OH) do not migrate far from the active centres on TiO_2, with catalytic degradation taking place essentially at the catalyst/water interface (Minero *et al*. 1992). Furthermore, the intermediates produced during degradation can also be adsorbed by activated carbon and/or further oxidized to avoid the secondary pollution caused by these sub-products.

The aim of the present work was to investigate the application of carbon/titania composites with different loadings for the photodegradation of phenol, one of the most persistent aromatic compounds frequently found in wastewater. It was expected that studies of the textural features of the as-prepared catalysts, and the retention of the target pollutant in their porous network, would enable the determination of the contribution of the adsorption process on the carbon-based composites to the overall photodegradation reaction. The results thus obtained would then enable the formulation of the best conditions for the preparation of such carbon-supported catalysts.

2. EXPERIMENTAL

2.1 Sample preparation

A commercial activated carbon AC (particle size 0.212–0.710 mm), obtained from the physical activation of coal, was used as the catalyst support. This carbon was characterized by a low oxygen content (2.1 wt%) and a basic nature (pH_{pzc} = 8.9). The titania/carbon catalysts were prepared by infiltration of a suspension of titanium oxide (P25 Degussa, 80% anatase and 20% rutile) in ethanol into the carbon material by means of a rotary evaporator under vacuum for 2 h, followed by evaporation of the solvent. The samples were labelled as ACTix, with "x" being the percentage of titanium oxide immobilized on the carbon support. Unimpregnated TiO_2 was used as a standard for comparison purposes. Before use, all samples were washed in distilled water at 60 ºC, dried at 110 ºC overnight and stored in a desiccator.

2.2. Characterization

The nano-texture of both the carbon support and the titania/carbon composites was characterized by nitrogen adsorption isotherms measured at –196 ºC (ASAP 2020 instrument, Micromeritics Instrument Corp., Norcross, GA, U.S.A.). Before such experiments, the samples were outgassed under vacuum (ca. 10^{-3} Torr) overnight at 120 ºC. The resulting isotherms were used to calculate the specific surface areas, S_{BET}, and pore volumes by applying the DFT method assuming a slit-shaped pore geometry. The samples were further characterized by thermogravimetric analysis (Setaram Labsys) employing the following instrument settings: heating rate of 15 ºC/min; nitrogen atmosphere at a flow rate of 50 mℓ/min. The point of zero charge was evaluated by the mass titration method as described elsewhere (Ania *et al*. 2007).

X-Ray diffraction (XRD) patterns were recorded on a Bruker D8 Advance instrument operating at 40 kV and 40 mA, and using Cu Kα (λ = 0.15406 nm) radiation. UV–vis diffuse reflectance spectra (DRS) were recorded on a Shimadzu spectrometer equipped with an integrating sphere

using $BaSO_4$ as a blank reference. The energy band gap widths of the catalysts were determined using the Kubelka–Munk methodology as described by Murphy (2007).

2.3. Adsorption and photodegradation of phenol

Kinetic experiments designed to examine the adsorption and photo-oxidation of phenol were undertaken under the same experimental conditions, employing batch methods at room temperature. Details of such experiments have been reported elsewhere (Velasco *et al*. 2010). Briefly, ca. 1 g/ℓ of adsorbent was placed in each of a series of glass flasks containing 400 mℓ of phenol solution (in distilled non-buffered water) at an initial concentration of 100 mg/ℓ and a pH of 6. The suspensions were stirred at 500 rpm with small aliquots of the solution (ca. 1 mℓ) being removed at fixed time intervals, filtered through cellulose filters (mean pore size = 0.45 μm) and analyzed by reverse-phase HPLC (Spherisorb C18, 125 mm × 4 mm) using methanol/water mixtures as the mobile phase and employing a photodiode array detector. For the photocatalytic tests, UV irradiation was provided by a high-pressure mercury lamp (125 W) suspended vertically in a cylindrical, double-walled quartz jacket cooled by flowing water (water cell) and immersed in the centre of the solution. The water cell was used to control the temperature during the experiments, thereby preventing any overheating of the suspension due to irradiation. All experiments were performed in duplicate, the average experimental error being < 5%.

3. RESULTS AND DISCUSSION

3.1. Characterization of the catalysts

Textural characterization of the different catalysts was carried out by means of nitrogen adsorption isotherms measured at –196 ºC [see Figure 1(a)]. The main textural parameters are listed in Table 1. P25 is a non-porous material which displays a Type II isotherm (Brunauer *et al*. 1940), as opposed to the Type I isotherm of the activated carbon which is characteristic of a highly microporous material. The isotherm for AC gradually changed towards a hybrid I/IV shape with immobilization of P25, indicating that the resulting carbon/titania (C/TiO_2) composites inherited the textural properties of both precursors.

The surface areas and pore volumes of the catalysts increased as the loading of titania decreased (Table 1), which was not unexpected considering the characteristics of P25 and AC. In fact, stoichoimetric (theoretical) calculations of the textural parameters of the catalysts taking account of the titania loading and the characteristics of both precursors fitted perfectly with the values obtained experimentally [Figure 1(b)]. In addition, an analysis of the pore-size distributions of the catalysts (not shown) revealed that a homogeneous and proportional fall in volume occurred for all pore sizes, rather than blockage of certain pore sizes. The absence of a constriction/enlargement of the mean pore size is in good agreement with the observed trend for the stoichiometric and experimental values for the surface areas and pore volumes.

These results suggest that immobilization of titania on the activated carbon occurred mainly on the outer surface. Consequently, the microporosity of the resulting hybrid catalysts should remain accessible during the adsorption and photo-oxidation tests. This is of great importance since the micropores are considered to be the active sites for the adsorption of aromatic molecules. Similar observations have been reported for activated carbon/titania composites with loadings > 50% prepared using a similar procedure (Araña *et al*. 2003a); in contrast, the in-situ preparation of

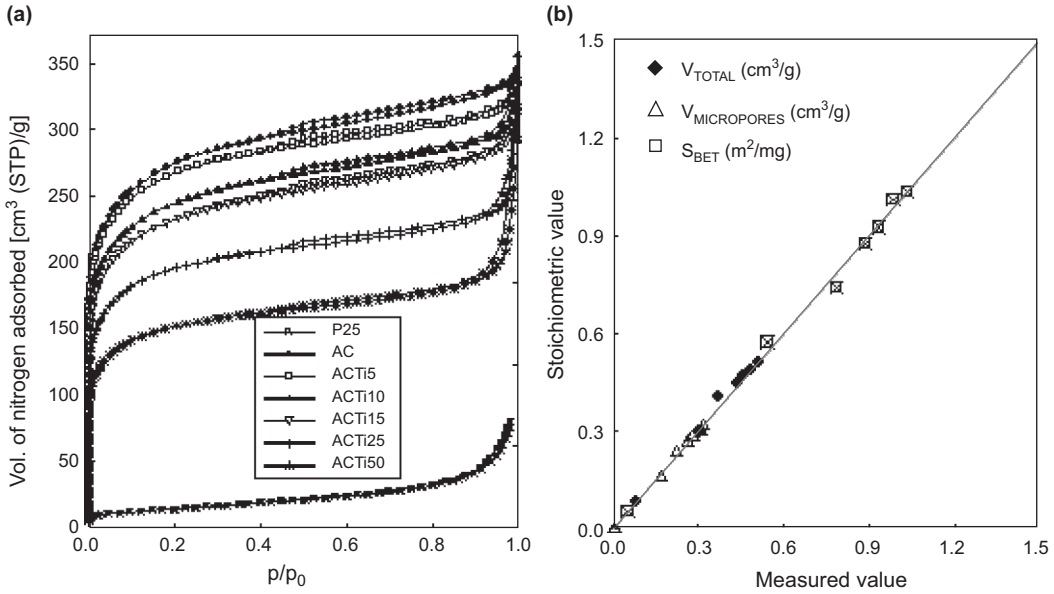

Figure 1. (a) Nitrogen adsorption isotherms of the studied materials measured at –196 ºC. (b) Relationship between the stoichiometric and measured textural parameters.

TABLE 1. Textural Parameters of the Carbon/Titania Composites Studied

Sample	S_{BET} (m^2/g)	V_{TOTAL}[a] (cm^3/g)	$V_{MICROPORES}$[b] (cm^3/g)	$V_{MESOPORES}$[b] (cm^3/g)
P25	53	0.083	–	–
ACTi5	1008	0.485	0.310	0.066
ACTi10	924	0.458	0.280	0.065
ACTi15	876	0.439	0.264	0.062
ACTi25	739	0.371	0.223	0.044
ACTi50	573	0.304	0.170	0.042

[a]Evaluated at a relative pressure of 0.95.
[b]Evaluated by the DFT method applied to the nitrogen adsorption data.

titania in the presence of a porous material (i.e. activated carbon) has been reported to block the pore features of the support (Tryba *et al*. 2003; Wu *et al*. 2008).

The XRD patterns of the studied catalysts are shown in Figure 2. The patterns corresponding to P25 show the well-defined peaks associated with the crystalline phases of anatase (25.3º) and rutile (27.4º), which were both present in the solid. The relative intensities of both peaks confirm that anatase was the dominant phase. In the case of the activated carbon, the patterns show broad peaks at 25º and 44º, corresponding to the (002) and (100) reflections associated with the presence

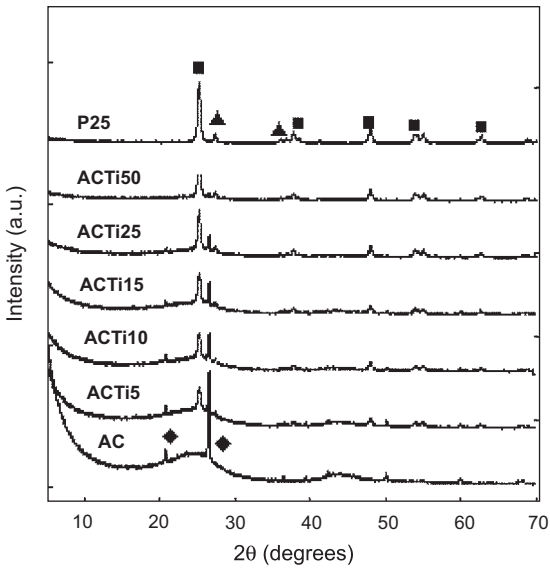

Figure 2. X-Ray diffraction patterns of the C/TiO_2 composites studied. Peak markings correspond to the following: ◆, SiO_2; ■, anatase; ▲, rutile.

of graphitic structures. In addition to these broad peaks typical of carbon materials, two sharp peaks at 2θ values of ca. 21º and ca. 27º, characteristic of silica (quartz phase), may be observed. Such peaks arise from the mineral matter of the activated carbon (ca. 11 wt%), as confirmed by chemical analysis and the XRD pattern of the as-received carbon material. The C/TiO_2 composites showed XRD patterns similar to those of the two precursors, although the intensities of the peaks were proportional to the titania and/or carbon loadings. This shows that all the carbon/titania catalysts possessed the same crystalline structure, regardless of the titania loading on the surface (low or high), and that immobilization of titanium oxide on the activated carbon did not alter the crystalline phases of the inorganic oxide.

The diffuse reflectance spectra of the catalysts are shown overleaf in Figure 3. The spectrum of P25 clearly shows the characteristic absorption edge of the anatase form of TiO_2 (predominant in P25) with the highest absorption in the UV region. The corresponding energy band gap evaluated for P25 was 3.16 eV, which is in good agreement with the values reported in the literature for this compound (Grzechulska and Morawski 2003; Nagaveni *et al*. 2004).

The absorption of visible light was pronounced for the C/TiO_2 composites due to the presence of the carbon, but the absorption edge in the UV region due to TiO_2 became ambiguous, thereby making an accurate calculation of the band gap energy difficult. This may be understood as due to the overlapping of the corresponding spectra of carbon and titania, where UV and visible light absorption are respectively suppressed and increased with the carbon content. Although having a low intensity, the absorption edge could be observed for the C/TiO_2 samples, with a slight shift to higher wavelength regions compared to bare TiO_2. This became more evident as the titania loading decreased, indicating a correlation between the AC content and the change in the UV adsorption spectra. This contrasts with previous work reported in the literature for composites with much lower carbon contents, where no correlation appeared to exist (Araña *et al*. 2003a). These results demonstrate the ability of the C/TiO_2 composites to absorb at wavelengths close to

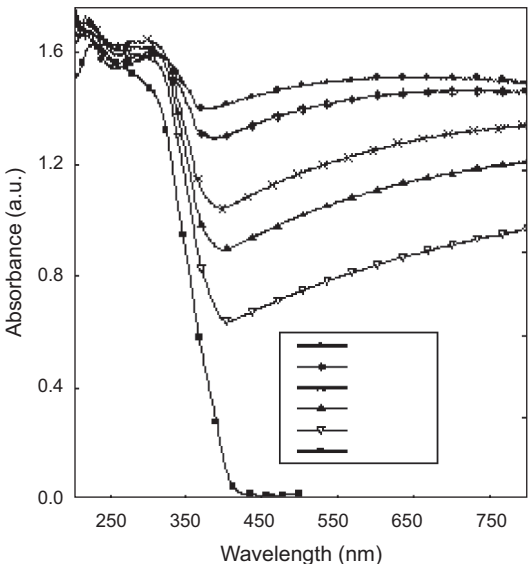

Figure 3. Diffuse reflectance spectra of the studied materials.

that of visible radiation, and that UV light was capable of passing through the carbon layer to excite the semiconductor particles, although the intensity of the radiation that reached the photoactive titania would be expected to be weakened.

3.2. Phenol adsorption

One of the advantages of immobilizing a catalyst on a porous support is the increase in the reaction rate. This is a direct consequence of the usually high specific surface area and pore volume of the support, which favour the confinement (adsorption) of the target species in the porosity of the support. Such positive confinement effects in porous substrates have been reported as enhancing the stability and activity of catalysts, and have been experimentally observed and theoretically confirmed (Ravindra *et al*. 2004). The improvement in activity is believed to be the result of enhanced interactions between the substrate and the immobilized catalyst (Chong and Zhao 2004). Thus, a close match between the pore size of the support and the molecular dimensions of the catalyst are known to be a crucial aspect for the improvement of the activity of the immobilized catalyst. However, diffusion barriers may be imposed on the system if the porosity of the support remains blocked after such immobilization. For this reason, we have explored the adsorption rate and capacity of an activated carbon loaded with different amounts of titania. The activity of the C/TiO_2 catalysts towards phenol photo-oxidation has also been explored.

Figure 4(a) shows the adsorption rate of phenol onto the series of C/TiO_2 composites, while Figure 4(b) shows the rate of phenol removal under UV irradiation of the composites (adsorption + photo-oxidation); in both cases, the data corresponding to bare titania are also depicted. As expected for a non-porous solid, the amount of phenol adsorbed onto P25 was very low (ca. 3%). For the C/TiO_2 composites, the amount adsorbed decreased with increasing titania content, which is consistent with the observed trend for the porosity of the catalysts. The higher the surface areas

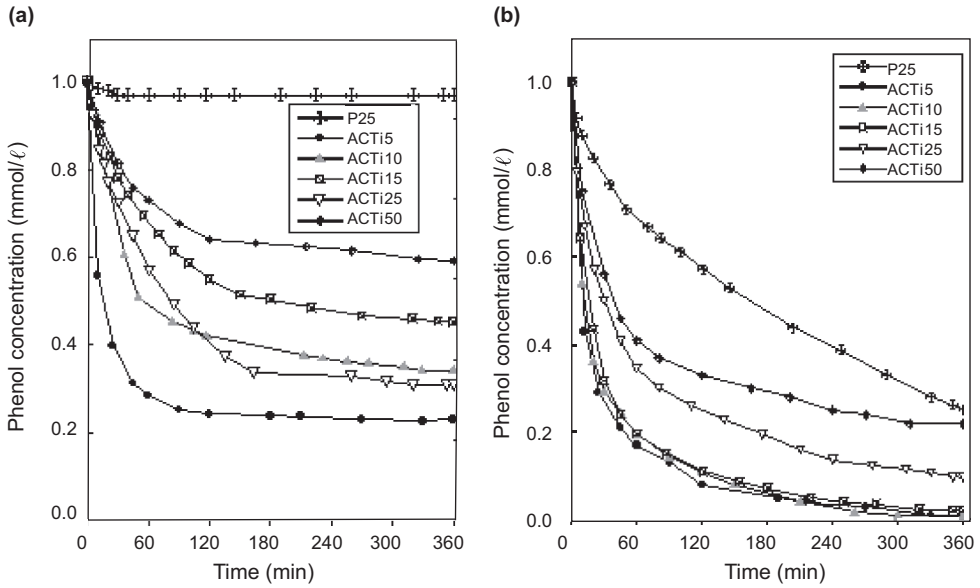

Figure 4. Kinetics of (a) phenol adsorption and (b) phenol removal under UV irradiation on the prepared C/TiO_2 composites.

and pore volumes of the C/TiO_2 catalysts, the higher the phenol uptake. Equally, the rate of adsorption also appears to be linked to the porosity of the catalysts. Various kinetic models were applied to fit the experimental kinetic data and in all cases the best fitting was obtained with the pseudo-second-order model (Ho 2006). The values of the pseudo-second-order rate constant for phenol adsorption ($k'_{2,\,ads.}$) decreased as the titania loading of the composites increased (Figure 5), with the exception of the samples ACTi25 and ACTi50 which showed similar values despite their

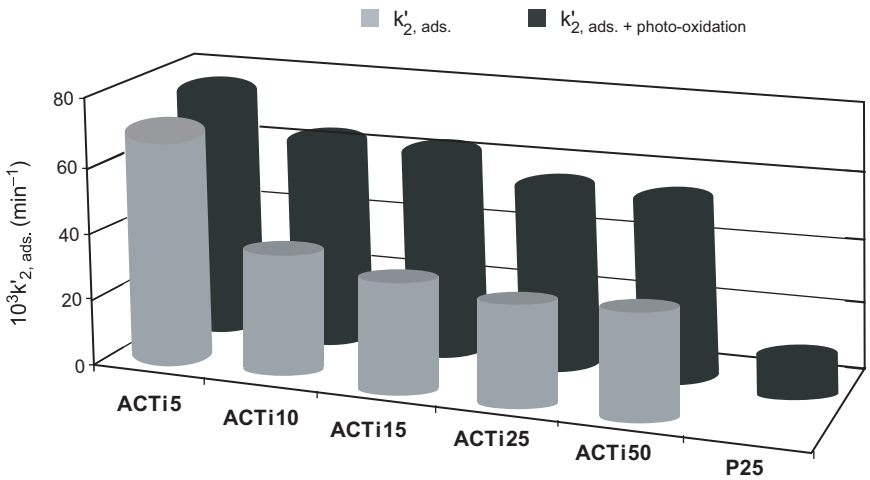

Figure 5. Evolution of kinetic rate constants for phenol adsorption ($k'_{ads.}$) and photo-oxidation ($k'_{ads.\,+\,photo\text{-}oxidation}$) on the prepared C/$TiO_2$ composites.

different TiO_2 content. It would thus appear that, as a general rule, both the phenol uptake and the adsorption rate were strongly dependent on the accessible porosity of the catalysts. The different behaviour observed for the samples with the highest P25 content might be linked to some operational problems which arose during its handling. Thus, some separation of the two components (inorganic/carbon) was observed upon immersion of the composite in solution; such a separation of titania particles from the carbon support would then modify the accessible porosity of the composite, which would also affect the adsorption kinetics (Figures 4 and 5). On the basis of this observation, it may be inferred that titania loadings above 20 wt% made the corresponding composites unsuitable for use in aqueous solution.

On the other hand, thermal analysis of the composites after phenol adsorption (Figure 6) allowed the active sites for phenol adsorption to be investigated. The DTG profiles show a first

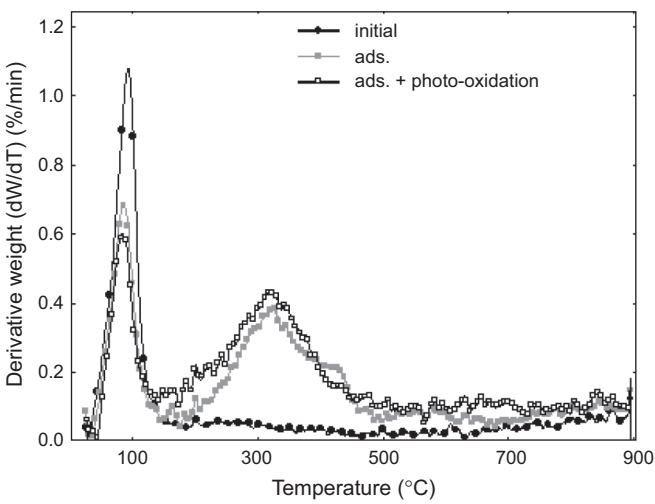

Figure 6. DTG profiles of sample ACTi10 after phenol adsorption (ads.) and UV irradiation (ads. + photo-oxidation).

desorption peak centred at 100 ºC, corresponding to the removal of the moisture retained in the materials; the second peak at ca. 300 ºC was due to desorption of the phenol retained in the low-energy adsorption sites of the catalysts (physisorption), as confirmed by MS spectrometry. A weak hump was also observed at ca. 425 ºC which was attributed to desorption of the chemisorbed fraction of phenol which showed a stronger interaction with the carbon matrix. Similar desorption profiles showing several peaks for phenol adsorption sites with different natures have been reported for activated carbons elsewhere (Ania *et al*. 2005; Toth *et al*. 2009). Based on the relative intensities of both peaks, it may be inferred that physisorption was favoured over chemisorption for all the composites at low solution concentrations of phenol.

In addition, it is interesting to point out that the peaks corresponding to the temperature for the maximum desorption of phenol remained constant despite the increasing titania loading of the catalysts. This confirms that the presence of P25 on the activated carbon did not substantially change the phenol adsorption sites on the carbon matrix; only the amount of phenol adsorbed diminished when the pore volume of the catalyst decreased. These results are in good agreement with the observed trend for the pore-size distributions of the materials, and also with the expected

mechanism for phenol adsorption in terms of the chemical properties of the composites. Indeed, from the magnitude of the dissociation constant for phenol ($pK_a \sim 9.71$), the neutral molecule would be the main entity in solution at the pH employed (ca. 6.5 for non-buffered solutions), being greater than 99 mol%. After the incorporation of titania, the composites showed pH_{pzc} values close to the solution pH, indicating that the surfaces of the composites did not charge during the adsorption experiments. Consequently, the retention of phenol on the investigated catalysts would not be expected to be affected by electrostatic interactions, and that the adsorption rate would be governed by dispersive forces (van der Waals) and the affinity of the phenol molecules for the catalyst surface.

3.3. Photo-oxidation of phenol under UV irradiation

Figure 4(b) shows the kinetics of phenol conversion when the prepared C/TiO_2 composites were exposed to UV irradiation, the photo-activity of the prepared catalysts being compared to that of non-supported P25 regarded as a reference catalyst. The non-catalyzed reaction (phenol photolysis under direct UV irradiation) was not considered further since although it promoted phenol conversion to aromatic intermediates, mineralization of the solution was not attained (i.e. the total organic carbon content of the solution before and after UV illumination remained unchanged).

It may be observed that, under UV light, the rate of phenol removal (photo-oxidation + adsorption) largely increased when P25 was immobilized in the activated carbon. For example, the final overall yield after irradiating for 6 h was 75% for P25 compared to over 95% for the C/TiO_2 composites. This tendency was more pronounced for composites with the lowest titania content (high carbon content), particularly during the early stages of the process. Although similar observations on the enhanced photo-activity of immobilized titania on a porous support have been reported previously (Tryba *et al*. 2003; Keller *et al*. 2005; Velasco *et al*. 2010; Araña *et al*. 2003a,b), most of the studies reported in the literature investigated higher titania loadings.

Our results show that even though the photocatalytic activity of titania particles seemed to be enhanced upon their immobilization on a porous carbon support, the overall disappearance of phenol from solution [Figure 4b)] seemed to be favoured by low titania loadings on the activated carbon support (ca. 10–15 wt%). Enhancement of the kinetics of phenol disappearance on UV irradiation of the C/TiO_2 composites may be explained in terms of the simultaneous adsorption of phenol into the catalyst pores and the degradation caused by the photo-activity of the immobilized TiO_2 particles. Thus, during the adsorption process, phenol molecules are transferred from the solution to the inner pores of the composites, thereby facilitating contact with the TiO_2 particles which are expected to be located on the outer surfaces of the C/TiO_2 catalysts.

Langmuir–Hinshelwood (L–H) kinetics given by the simplified apparent first-order model (Kumar *et al*. 2008) were first applied to the experimental data for phenol removal under UV illumination. However, it was found that the dependence of the logarithmic ratio of concentration on time was not linear, thereby indicating that the system under study did not follow pseudo-first-order kinetics. For this reason, the pseudo-second-order kinetic model was employed to fit the experimental data. The pseudo-second-order kinetic rate law may be expressed by the equation (Zainal *et al*. 2007):

$$\frac{dQ_t}{dt} = k'_{2,\,\text{ads.}\,+\,\text{photo-oxidation}}\left(Q_0 - Q_t\right)^2$$

which can be expressed in a linear fashion as:

$$\frac{t}{Q_t} = \frac{1}{k'_{2,\text{ ads. + photo-oxidation}} Q_0^2} + \left(\frac{t}{Q_0}\right)$$

where Q_0 is the initial amount of pollutant, Q_t is the amount of pollutant eliminated at time t and $k'_{2\text{ ads. + photo-oxidation}}$ is the apparent removal rate constant. A linear dependence between t/Q_t and time would allow the apparent rate constant for simultaneous adsorption and photo-oxidation to be evaluated from the intercept of the corresponding plot.

Figure 5 depicts a histogram of the apparent removal rate constants ($k'_{2,\text{ ads + photo-oxidation}}$) plotted against those obtained for the corresponding adsorption process ($k'_{2,\text{ ads.}}$) Some differences between the kinetic process involved in phenol adsorption and removal under UV irradiation may be clearly observed. Compared to the situation in the absence of UV irradiation, the rate of phenol disappearance on irradiating the C/TiO_2 composites largely increased with the carbon content. This trend was more evident during the initial stages of the reaction (short times). After irradiation for 6 h, phenol was almost completely removed from aqueous solution by the C/TiO_2 composites with a P25 loading in the range 5–15 wt%.

Equally, the nature of the photo-oxidation intermediates detected in solution also appeared to depend on the titania content of the composites. Thus, the chemical composition of the intermediates appearing during the photo-oxidation experiments in the presence of the different catalysts was determined by reverse-phase HPLC (Figure 7). However, the presence of non-aromatic intermediates (such as organic acids with short alkyl chains) was not evaluated, since they could not be detected by the analytical technique used to identify, separate and quantify the intermediates. Further studies are ongoing on this topic and will be the subject of future reports.

The data depicted in Figure 7 indicate that increasing amounts of *p*-benzoquinone (BZ), hydroquinone (HY) and catechol (CAT) were detected when P25 was irradiated. This finding is in good agreement with the results reported by Azevedo *et al*. (2009) for Degussa P25. Compared with the results obtained for the C/TiO_2 samples, higher concentrations of intermediates were found when bare TiO_2 was irradiated. However, since P25 is a non-porous material, it should be noted that all the degradation sub-products were not necessarily detected in the solution in this case.

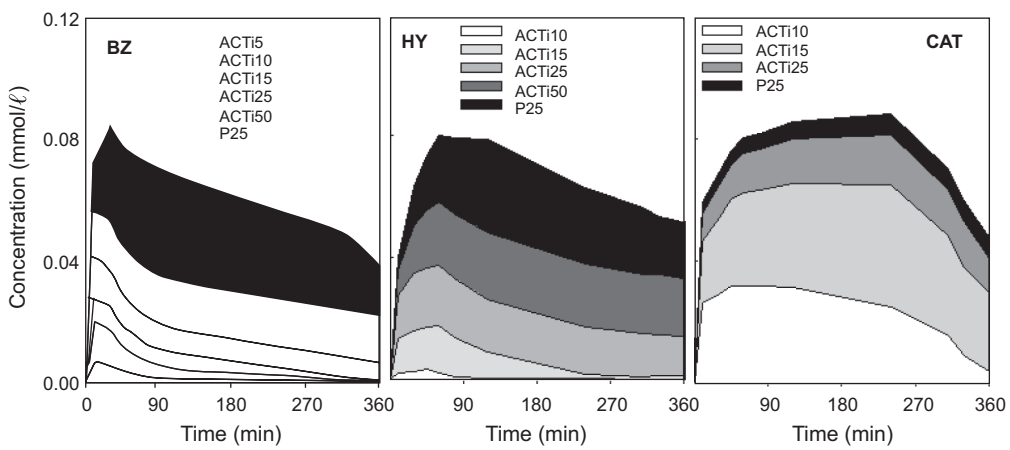

Figure 7. Evolution of photo-oxidation intermediates with time upon UV irradiation of the C/TiO_2 composites.

With the C/TiO_2 composites, a fraction of the degradation compounds would be expected to be retained (adsorbed) inside the carbon matrices due to their porous features. Nevertheless, the DTG profiles of the composites after UV irradiation (Figure 6) did not show any significant differences relative to those obtained after adsorption. This suggests that the photo-oxidation intermediates (if any) could have been retained on the adsorption sites identified for phenol, which is not unreasonable when the similar chemical characters of phenol and most of its aromatic degradation intermediates are taken into account.

As a general trend, the amount of aromatic intermediates detected in the solution increased with the titania loading of the composites, being greatest for P25 itself (BZ and HY). Thus, for example, only traces of benzoquinone were detected upon irradiation of ACTi5. Of further importance is the large amount of catechol detected for C/TiO_2 composites with low titania loadings (i.e. ACTi10 and ACTi15), suggesting the preferential formation of catechol over benzoquinone and hydroquinone. According to the literature, the conversion of phenol to catechol facilitates its complete adsorption rather than allowing its conversion to benzoquinone or hydroquinone (Santos *et al*. 2002). An efficient photocatalyst should promote the formation of this compound, but also lead to a fast and high removal of the target pollutant and allow for its easy recovery from the solution. On this basis, it may be concluded that, of the samples studied, C/TiO_2 composites containing ca. 10–15 wt% titania were those most suitable for the removal and photo-oxidation of phenol from aqueous solutions.

4. CONCLUSIONS

Highly efficient activated carbon/titania photocatalysts with a low titanium oxide (P25) content have been prepared and applied to the removal of phenol from aqueous solutions. The rate of phenol adsorption increased when P25 was immobilized on the carbon support. Thus, phenol uptake was very fast for samples containing ca. 10–15 wt% titanium oxide due to the absence of mass-transfer limitations on the accessibility of the pollutant from the bulk solution to the titania/support interface. In contrast, titania loadings above 20 wt% led to operational problems that prevent the application of the corresponding catalysts in aqueous solutions.

Those C/TiO_2 composites which exhibited higher adsorption rates in the absence of UV illumination also exhibited a faster rate of phenol disappearance in the presence of UV light, along with the formation of lower amounts of intermediates. Removal efficiencies close to 100% were obtained for C/TiO_2 composites with low titanium oxide contents, together with the preferential oxidation of phenol to catechol. The improved performance of C/TiO_2 composites with low titania loadings may also be connected to the observed enhancement in the fraction of visible light absorbed by these composites, relative to the spectrum exhibited by bare titania.

The best photocatalysts are expected to facilitate the complete adsorption of phenol while maintaining a rapid and high removal extent. Thus, the C/TiO_2 composites containing ca. 10–15 wt% titania were found to be the most suitable materials for the removal and degradation of phenol from aqueous solution. This represents a clear advantage for any large-scale implementation of this process, since the improved separation of the catalyst together with its recycling and re-use during several cycles would be expected.

ACKNOWLEDGEMENTS

The authors acknowledge the support of the Spanish MICINN (CTM2008-01956). LFV thanks CSIC for a pre-doctoral fellowship. COA thanks CSIC for financial support (200980I131).

REFERENCES

Ania, C.O., Cabal, B., Parra, J.B. and Pis, J.J. (2007) *Adsorpt. Sci. Technol.* **25,** 155.
Ania, C.O., Parra, J.B., Pevida, C., Arenillas, A., Rubiera, F. and Pis, J.J. (2005) *J. Anal. Appl. Pyrolysis* **74,** 518.
Araña, J., Doña-Rodrıguez, J.M., Tello Rendón, E., Garriga i Cabo, C., González-Dıaz, O., Herrera-Melián, J.A., Pérez-Peña, J., Colón, G. and Navio, J.A. (2003a) *Appl. Catal. B* **44,** 161.
Araña, J., Doña-Rodrıguez, J.M., Tello Rendón, E., Garriga i Cabo, C., González-Dıaz, O., Herrera-Melián, J.A., Pérez-Peña, J., Colón, G. and Navio, J.A. (2003b) *Appl. Catal. B* **44,** 153.
Azevedo, E.B., Torres, A.R., Aquino Neto, F.R. and Dezotti, M. (2009) *Braz. J. Chem. Eng.* **26,** 75.
Bideau, M., Claudel, B., Dubien, C., Faure, L. and Kazouan, H. (1995*) J. Photochem. Photobiobiol. A* **91,** 137.
Brunauer, S., Deming, L.S., Deming, W.E. and Teller, E. (1940) *J. Am. Chem. Soc.* **62,** 1723.
Chong, A.S.M. and Zhao, X.S. (2004) *Catal. Today* **93,** 293.
Fernández, A., Lassaletta, G., Jiménez, V.M., Justo, A., Gonzàlez-Elipe, A.R., Herrmann, J.M., Tahiri, H. and Ait-Ichou, Y. (1995) *Appl. Catal. B* **7,** 49.
Grzechulska, J. and Morawski, A.W. (2003) *Appl. Catal. B* **46,** 415.
Ho, Y.S. (2006) *J. Hazard. Mater. B* **136,** 681.
Keller, N., Rebmann, G., Barraud, E., Zahraa, O. and Keller, V. (2005) *Catal. Today* **101,** 323.
Kumar, K.V., Porkodi, K. and Rocha, F. (2008) *Catal. Commun.* **9,** 82.
Matos, J., Laine, J. and Herrmann, J.-M. (2001) *J. Catal.* **200,** 10.
Matos, J., Laine, J., Herrmann, J.-M., Uzcategui, D. and Brito, J.L. (2007) *Appl. Catal. B* **70,** 461.
Minero, C., Catozzo, F. and Pelizzetti, E. (1992) *Langmuir* **8,** 481.
Mohseni, M. (2005) *Chemosphere* **59,** 335.
Murphy, A.B. (2007) *Sol. Energy Mater. Sol. Cells* **91,** 1326.
Nagaveni, K., Hegde, M.S., Ravishankar, N.G., Subbanna, N. and Madras, G. (2004) *Langmuir* **20,** 2900.
Pelizzetti, E. and Serpone, N. (Eds) (1989) *Photocatalysis: Fundamental and Applications*, Wiley, New York.
Ravindra, R., Zhao, S., Gies, H. and Winter, R. (2004) *J. Am. Chem. Soc.* **126,** 12 224.
Santos, A., Yustos, P., Quintanilla, A., Rodríguez, S. and Garcia-Ochoa, F. (2002) *Appl. Catal. B* **39,** 97.
Toth, A., Novak, C. and Laszlo, K. (2009) *J. Therm. Anal. Calorim.* **97,** 273.
Tryba, B., Morwski, A.W. and Inagaki, M. (2003) *Appl. Catal. B* **41**, 427.
Velasco, L.F., Parra, J.B. and Ania, C.O. (2010) *Appl. Surf. Sci.* **256,** 5254.
Wu, C.H., Shr, J.F., Wu, C.F. and Hsie, C.T. (2008*) J. Mater. Process. Technol.* **203,** 326.
Zainal, Z., Lee, C.Y., Hussein, M.Z., Kassim, A. and Yusof, N.A. (2007) *J. Hazard. Mater.* **146,** 73.